30th Annual International IEEE EMBS Conference
Vancouver, British Columbia, Canada, August 20-24, 2008

Advanced MR Diffusion Characterization of Neural Tissue Using Directional Diffusion Kurtosis Analysis

Edward S. Hui, Matthew M. Cheung, Liqun Qi and Ed X. Wu*

Abstract—**MR Diffusion kurtosis imaging (DKI) was proposed recently to study the deviation of water diffusion from Gaussian distribution. Mean kurtosis (MK), directionally averaged kurtosis, has been shown to be useful in assessing pathophysiological changes. However, MK is not sensitive to kurtosis change occurring along a specific direction. Therefore, orthogonal transformation of the 4th order kurtosis tensor was introduced in the current study to compute kurtoses along the 3 eigenvector directions of the 2nd order diffusion tensor. Such axial ($K_{//}$) and radial ($K_{\perp}$) kurtoses measured the kurtoses along the directions parallel and perpendicular, respectively, to the principal diffusion direction. DKI experiments were performed in normal adult and formalin-fixed rat brain, and developmental brains. The results showed that directional kurtosis analysis revealed different information for tissue characterization.**

Index Terms—**Directional kurtosis, diffusion kurtosis tensor, restricted diffusion, and orthogonal transformation.**

I. Introduction

Diffusion kurtosis imaging (DKI) was recently proposed to characterize non-Gaussian water diffusion behavior in neural tissues [1, 2]. Neuronal tissues are known to be heterogeneous in nature and comprises multiple compartments [3]. Thus the Gaussian distribution generally assumed for free water diffusion is insufficient to describe the biological diffusion process [4]. In addition, the dependency of diffusion-weighted (DW) signal on b-value has been observed to be non-monoexponential [5]. To characterize such non-Gaussian diffusion behavior, kurtosis, the 4th central moment of a distribution [6], was introduced [1]. Positive kurtosis indicates that a distribution is more sharply peaked than Gaussian, indicative of a more restricted diffusion environment. Apparent diffusion kurtosis has been estimated by acquiring DW signals at multiple b-values up to a maximum of 2500 s/mm^2 in humans [1, 2]. Because the 4th order diffusion kurtosis tensor (KT) has 15 independent components, DKI experiments are typically performed in more than 15 directions to estimate the full KT.

Recent experimental findings in human DKI studies were promising [1, 2, 7-9]. Mean kurtosis (MK), the average apparent kurtosis along all diffusion encoding directions, was measured and shown to offer an improved sensitivity in detecting developmental and pathological changes in neural tissues as compared to the conventional diffusion tensor imaging (DTI). However, taking the mean of apparent kurtoses measured along all encoding directions would reduce the sensitivity and specificity in probing kurtosis change occurring along a specific direction, for instance, parallel or perpendicular to the principal diffusion eigenvector denoted as axial or radial direction, respectively. Given that directional diffusivity analyses have been successfully employed to elucidate specific neural tissue pathologies in animal models [10, 11] and humans [12], it is valuable to analyze directional kurtoses by obtaining kurtoses along these two directions. Such directional kurtosis analysis may provide different information regarding MR diffusion characterization of neural tissues in normal, developmental or pathological states.

In this study, an orthogonal transformation of the 4th order KT was proposed to compute kurtoses along the directions of the three diffusion eigenvectors. Histological fixation and brain development are known to alter the cellular structure and hence the restriction to water diffusion [13-15], likely leading to varying extents of water diffusion restriction along the axial and radial directions. Therefore, DKI experiments were performed in both normal and formalin-fixed adult rat brains, and 13-day-postnatal rats (P13) to document both DKI and DTI measurements in various brain tissues, and to evaluate whether directional kurtosis analysis improves tissue characterization.

II. Materials And Methods

A. Theory

In conventional DTI, 2nd order diffusion tensor (DT) is fully characterized by its eigenvalues (λ_i with i=1,2,3 and $\lambda_1 > \lambda_2 > \lambda_3$) and the orthonormal eigenvectors [16]. In DKI

This work was supported in part by the University of Hong Kong CRCG grant and Hong Kong Research Grant Council grant.

Ed X. Wu, Edward S. Hui and Matthew M. Cheung are with the Laboratory of Biomedical Imaging and Signal Processing and the Department of Electrical and Electronic Engineering, The University of Hong Kong, Pokfulam, Hong Kong (phone: (852) 2819-9713; e-mail: ewu@eee.hku.hk).

Liqun Qi is with the Department of Applied Mathematics, The Hong Kong Polytechnic University, Hung Hom, Kowloon, Hong Kong.

[1, 2], both apparent diffusion coefficient (D_{app}) and apparent diffusion kurtosis (K_{app}) along each applied diffusion gradient direction are estimated by fitting the following equation with multiple DW signals acquired using a range of b-values:

$$\ln[S(b)/S(0)] = -bD_{app} + (1/6)b^2 D_{app}{}^2 K_{app}, \quad (1)$$

where S(b) is the DW signal intensity at a particular b-value, and S(0) is the signal without applying any diffusion gradient. To obtain reliable curve fitting, a sufficient b-value range must be chosen to permit as much non-monoexponential decay as possible. However, it must be before the occurrence of the minima in (1), after which the kurtosis model will fail.

The mean kurtosis (MK) is measured as:

$$MK = (1/n)\sum_{i=1}^{n}(K_{app})_i, \quad (2)$$

where $(K_{app})_i$ is the K_{app} along i^{th} direction and n is the total number of directions in which diffusion measurements are carried out. K_{app} at a particular direction is related to a 4^{th} order kurtosis tensor (KT) by:

$$K_{app} = (MD^2/D_{app}^2)\sum_{i=1}^{3}\sum_{j=1}^{3}\sum_{k=1}^{3}\sum_{l=1}^{3} n_i n_j n_k n_l W_{ijkl}, \quad (3)$$

where mean diffusivity is $MD = (1/3)\sum_{i=1}^{3}\lambda_i$, n_i the component of the encoding gradient unit vector and W_{ijkl} the individual element of KT. Note that KT has 15 independent elements only due to the symmetry of different processes probed by MR. Because of the mathematical complexity of the 4^{th} order tensor [17], individual KT elements, eigenvalues and eigenvectors are yet to be explored in terms of their direct physical relevance to the diffusion processes. Nevertheless, KT can be transformed from the standard Cartesian coordinate system to another coordinate system in which the 3 orthonormal eigenvectors of DT are the base coordinate vectors by [18]:

$$\hat{W}_{ijkl} = \sum_{i'=1}^{3}\sum_{j'=1}^{3}\sum_{k'=1}^{3}\sum_{l'=1}^{3} e_{i'i}e_{j'j}e_{k'k}e_{l'l}W_{i'j'k'l'}. \quad (4)$$

From (3) and (4), the kurtosis along the individual DT eigenvector is:

$$K_i = (MD^2/\lambda_i^2)\hat{W}_{iiii}. \quad (5)$$

Thus the axial ($K_{//}$) and radial kurtosis ($K_\perp$) can be obtained from the three newly derived kurtoses, i.e. $K_{//} = K_1$ and $K_\perp = (K_2 + K_3)/2$.

To examine the anisotropy of kurtoses, fractional anisotropy of kurtosis (FA_K) can also be conveniently defined in a way similar to that of conventional DTI [19] as:

$$FA_K = \sqrt{\frac{3}{2}\cdot\frac{(K_1-\overline{K})^2 + (K_2-\overline{K})^2 + (K_3-\overline{K})^2}{K_1{}^2 + K_2{}^2 + K_3{}^2}}, \quad (6)$$

where $\overline{K} = (1/3)\sum_{i=1}^{3} K_i$.

B. In Vivo and Ex Vivo Rat Brain DKI

All MRI experiments were performed on a 7T scanner (Bruker). In vivo DKI was carried out on normal 10-month-old SD rats (N=7). DW images were acquired with a respiration-gated spin echo 4-shot EPI sequence in 30 gradient directions [20]. 5 additional images with b=0 were acquired. The sequence parameters were: TR/TE=3000/30.3ms, δ/Δ=5/17ms, slice thickness(TH)=1mm, NEX=4, data matrix=128x128 and image resolution 234x234μm^2. 5 b-values were used for each gradient direction (0.5, 1.0, 1.5, 2.0 and 2.5ms/μm^2). Such b-values were chosen to allow sufficient non-monoexponential decay of DW signals, but they were smaller than b_{minima} estimated from the mean kurtosis values reported in the previous human study [2].

For ex vivo DKI experiments, the brains of normal 10-month-old SD rats (N=5) were fixed and suspended by 1% agarose gel in plastic tubes for MRI at ~20°C. All acquisition parameters were the same as those for in vivo experiments except for the followings: TE/δ=34.3/9ms, and b-values of 1.0, 2.0, 3.0, 4.0 and 5.0ms/μm^2. Note that a larger b-value range was employed because the diffusivities in rodent brains decrease substantially under formalin fixation [21].

C. P13 Rat Brain DKI

P13 SD rats (N=6) were scanned with the same acquisition parameters as those for in vivo experiments except the followings: TE/δ/Δ=33.3/5/20ms, TH=0.7mm, image resolution 195x195μm^2 and NEX=2.

D. Data Analysis

DW signals were fitted to (1) for D_{app} and K_{app} along each diffusion direction following the procedures described earlier in [2]. MK, $K_{//}$, $K_\perp$ and FA_K maps were calculated. MD, FA, $\lambda_{//}$ and $\lambda_\perp$ maps [10] were also obtained for comparison. Multi-slice regions of interest (ROIs) were manually drawn on FA and MK maps by referencing to the standard rat brain atlas. 4 white matter (WM) tissues, namely CC, external capsule (EC), cerebral peduncle (CP) and anterior commissure (AC), and 3 gray matter (GM) tissues, namely cerebral cortex (CT), hippocampus (HP) and cauduate putamen (CPu) were defined.

III. Results

A. In Vivo and Ex Vivo Rat Brain DKI

Fig. 1 illustrated the typical MD, $\lambda_{//}$, $\lambda_\perp$, FA, MK, $K_{//}$, $K_\perp$ and FA_K maps from an intact in vivo rat brain and a formalin-fixed ex vivo rat brain. Interestingly, relatively less contrast was seen between WM and GM in vivo for $K_{//}$ map than ex vivo formalin-fixed condition. DTI and DKI measurements of various neural tissues were shown in Fig. 2. Dramatic significant reductions in MD, $\lambda_{//}$ and $\lambda_\perp$ were observed under formalin fixation for all GM and WM tissues with FA being largely preserved, consistent with the previous findings by others [22]. Significant kurtosis increase was observed for all WM and GM tissues under formalin fixation. Note that GM tissues exhibited relatively low kurtoses with $K_{//}$ and $K_\perp$ being similar. In addition, the trend of FA_K for different tissues in vivo and ex vivo was found to be similar to that of FA though it yielded a slightly narrower range. Fig. 3 showed the scatter plots in diffusivity- and kurtosis-space for

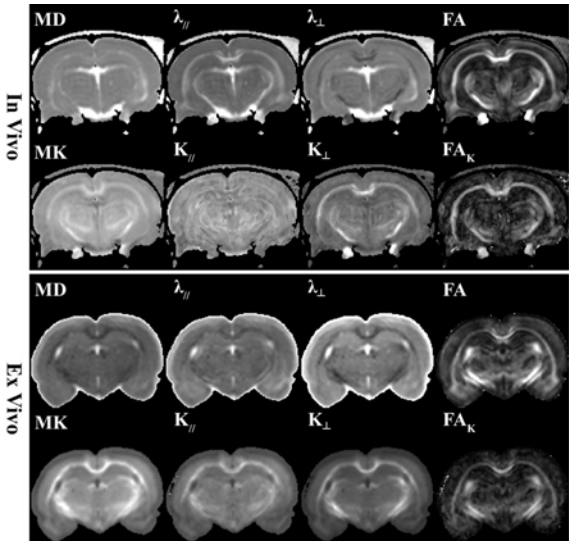

Fig. 1. MD, $\lambda_{//}$, $\lambda_{\perp}$, FA, MK, $K_{//}$, $K_{\perp}$ and FA_K maps of a typical in vivo and formalin-fixed ex vivo rat brain.

various tissues among all in vivo rat brain studied. GM tissues could be separated from WM tissues in both spaces. In particular, $K_{\perp}$ showed the best differentiating capability among all directional diffusivities and kurtoses, underscoring the usefulness of directional kurtosis analysis.

B. P13 and Adult Rat Brain DKI

Typical DTI- and DKI-derived maps of P13 rat brain were shown in Fig. 4. Measurements of different structures were

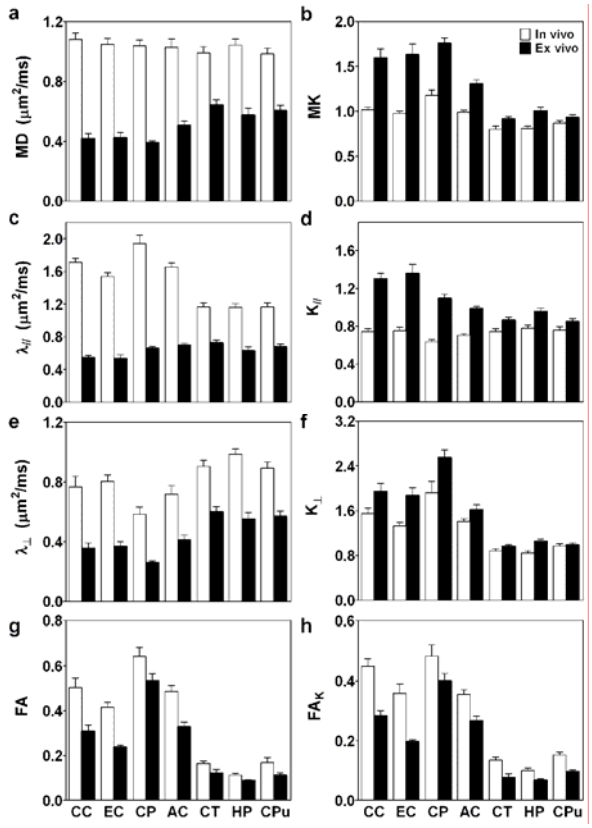

Fig. 2. DTI and DKI measurements of various neural tissues from in vivo adult rat brains (N=7) and formalin-fixed ex vivo adult rat brain samples (N=5).

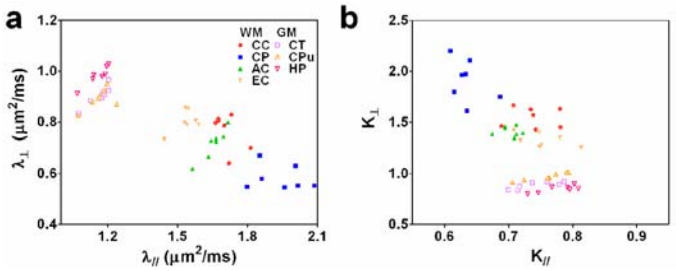

Fig. 3. Scatter plots of the directional diffusivities ($\lambda_{\perp}$ vs. $\lambda_{//}$) and directional kurtoses ($K_{\perp}$ vs. $K_{//}$) measured for various neural tissues from 7 in vivo brains

also shown in Fig. 5. It was found that there was significant increase in $K_{//}$ and $K_{\perp}$ from P13 to adult rat with $K_{\perp}$ having a much larger increase. Also note that WM generally showed larger change in kurtosis than GM.

IV. Discussions And Conclusions

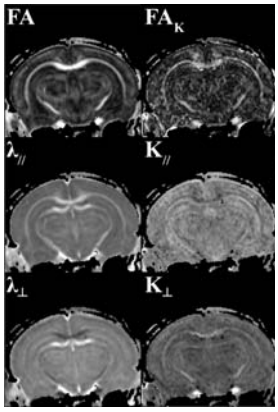

Fig. 4. FA, $\lambda_{//}$, $\lambda_{\perp}$, FA_K, $K_{//}$ and $K_{\perp}$ maps of a P13 rat brain.

In vivo water diffusion is a complex process with restriction incurred by numerous determinants such as intra-/extracellular compartments, permeability or water exchange, and potentially other biophysical properties associated with different water populations. Such biophysical complexity underscores the importance of investigating the restrictive diffusion environments in order to provide a more sensitive and specific MR characterization of neural tissues. With DKI, information regarding the extent of water diffusion restriction can then be obtained. With the directional kurtosis analysis performed in the current study, different and complimentary measurements were obtained indicating that such analysis can be used to enhance the characterization of normal and pathophysiological change in

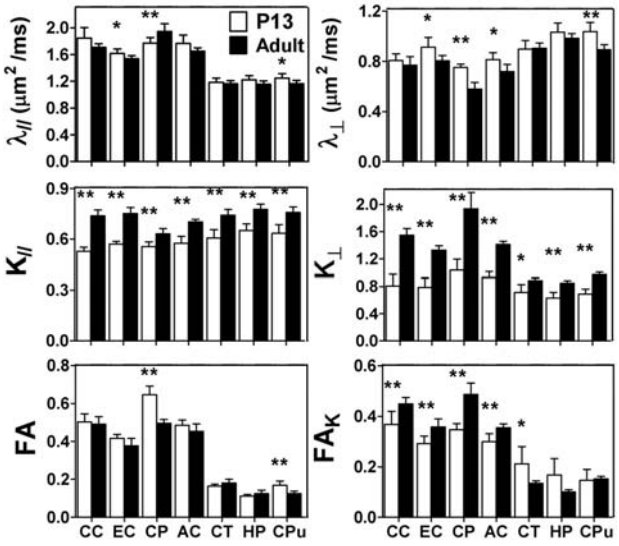

Fig. 5. DTI and DKI measurements of various neural tissues from normal P13 (N=6) and adult rat brain (N=7). * p<0.05, ** p<0.01.

neural tissues.

In vivo WM microstructure is often simplified as the ordered axons that contain neurofibrils such as microtubules and neurofilaments, which are wrapped by myelin [23]. As a result, one would expect the in vivo diffusion environment along the axonal direction could be rather homogeneous, thus leading to less diffusion restriction and lower $K_{//}$ than in GM. However, this was not the case. As shown in Fig. 2(d), WM and GM exhibited similar $K_{//}$ values in vivo. Such diffusion restriction in WM along the axonal or axial direction may be ascribed to the presence of membranes of the glial cells, astrocytes and oligodendrocytes [24]. It is worth noting that despite the general increase for all kurtosis indices, MK lacks the directional information that is useful in differentiating specific diffusion environment changes along axial and radial directions, .e.g., as revealed by the $K_{//}$ and $K_{\perp}$ above.

Our experimental data showed that kurtoses were found to be much more significantly sensitive to developmental changes than diffusivities (Fig. 5). Moreover, the increase in $K_{\perp}$ was found to be much higher than that of $K_{//}$, suggesting that there was more formation of barriers to water diffusion in the radial direction. Apart from myelination, microstructural environment changes in axon should also be taken into account.

In summary, directional kurtosis analysis in the current study shows promise in extracting more information regarding neuronal systems under pathophysiological or developmental changes in addition to conventional DTI.

ACKNOWLEDGMENT

The work was in part supported by Hong Kong Research Grant Council and HKU CRCG grants. The authors would like to thank Drs. Jens H. Jensen and Joseph A. Helpern at New York University School of Medicine in New York, and Dr. Hanzhang Lu at UT Southwestern Medical Center in Dallas for providing assistance with data processing procedures.

REFERENCES

[1] J. H. Jensen, J. A. Helpern, A. Ramani, H. Lu, and K. Kaczynski, "Diffusional kurtosis imaging: the quantification of non-gaussian water diffusion by means of magnetic resonance imaging," *Magn Reson Med,* vol. 53, pp. 1432-40, Jun 2005.

[2] H. Lu, J. H. Jensen, A. Ramani, and J. A. Helpern, "Three-dimensional characterization of non-gaussian water diffusion in humans using diffusion kurtosis imaging," *NMR Biomed,* vol. 19, pp. 236-47, Apr 2006.

[3] D. Le Bihan, "Molecular diffusion nuclear magnetic resonance imaging," *Magn Reson Q,* vol. 7, pp. 1-30, Jan 1991.

[4] J. Karger, "NMR Self-Diffusion Studies in Heterogeneous Systems," *Advances in Colloid and Interface Science,* vol. 23, pp. 129-148, 1985.

[5] R. V. Mulkern, H. Gudbjartsson, C. F. Westin, H. P. Zengingonul, W. Gartner, C. R. Guttmann, R. L. Robertson, W. Kyriakos, R. Schwartz, D. Holtzman, F. A. Jolesz, and S. E. Maier, "Multi-component apparent diffusion coefficients in human brain," *NMR Biomed,* vol. 12, pp. 51-62, Feb 1999.

[6] K. P. Balanda and H. L. Macgillivray, "Kurtosis - a Critical-Review," *American Statistician,* vol. 42, pp. 111-119, May 1988.

[7] M. F. Falangola, A. Ramani, A. Dl Martino, J. H. Jensen, J. S. Babb, C. Hu, K. U. Szulc, F. X. Castellanos, and J. A. Helpern, "Age-Related Patterns of Change in Brain Microstructure by Diffusional Kurtosis Imaging," In: Proceedings of the 15th Annual Meeting of ISMRM, Berlin, Germany, 2007, p. 667.

[8] J. A. Helpern, M. F. Falangola, A. Dl Martino, A. Ramani, J. S. Babb, C. Hu, J. H. Jensen, and F. X. Castellanos, "Alterations in Brain Microstructure in ADHD by Diffusional Kurtosis Imaging," In: Proceedings of the 15th Annual Meeting of ISMRM, Berlin, Germany, 2007, p. 1580.

[9] A. Ramani, J. H. Jensen, K. U. Szulc, O. Ali, C. Hu, H. Lu, J. D. Brodle, and J. A. Helpern, "Assessment of abnormalities in the cerebral microstructure of schizophrenia patients: a diffusional kurtosis imaging study," In: Proceedings of the 15th Annual Meeting of ISMRM, Berlin, Germany, 2007, p. 648.

[10] S. K. Song, S. W. Sun, M. J. Ramsbottom, C. Chang, J. Russell, and A. H. Cross, "Dysmyelination revealed through MRI as increased radial (but unchanged axial) diffusion of water," *Neuroimage,* vol. 17, pp. 1429-36, Nov 2002.

[11] S. W. Sun, H. F. Liang, K. Trinkaus, A. H. Cross, R. C. Armstrong, and S. K. Song, "Noninvasive detection of cuprizone induced axonal damage and demyelination in the mouse corpus callosum," *Magn Reson Med,* vol. 55, pp. 302-8, Feb 2006.

[12] S. A. Trip, C. Wheeler-Kingshott, S. J. Jones, W. Y. Li, G. J. Barker, A. J. Thompson, G. T. Plant, and D. H. Miller, "Optic nerve diffusion tensor imaging in optic neuritis," *Neuroimage,* vol. 30, pp. 498-505, Apr 1 2006.

[13] E. D. Schwartz, E. T. Cooper, C. L. Chin, S. Wehrli, A. Tessler, and D. B. Hackney, "Ex vivo evaluation of ADC values within spinal cord white matter tracts," *AJNR Am J Neuroradiol,* vol. 26, pp. 390-7, Feb 2005.

[14] M. Takahashi, D. B. Hackney, G. Zhang, S. L. Wehrli, A. C. Wright, W. T. O'Brien, H. Uematsu, F. W. Wehrli, and M. E. Selzer, "Magnetic resonance microimaging of intraaxonal water diffusion in live excised lamprey spinal cord," *Proc Natl Acad Sci U S A,* vol. 99, pp. 16192-6, Dec 10 2002.

[15] P. E. Thelwall, T. M. Shepherd, G. J. Stanisz, and S. J. Blackband, "Effects of temperature and aldehyde fixation on tissue water diffusion properties, studied in an erythrocyte ghost tissue model," *Magn Reson Med,* vol. 56, pp. 282-9, Aug 2006.

[16] P. J. Basser, J. Mattiello, and D. LeBihan, "MR diffusion tensor spectroscopy and imaging," *Biophys J,* vol. 66, pp. 259-67, Jan 1994.

[17] L. Q. Qi, "Eigenvalues of a real supersymmetric tensor," *Journal of Symbolic Computation,* vol. 40, pp. 1302-1324, Dec 2005.

[18] L. Qi, Y. Wang, and E. X. Wu, "D-eigenvalues of diffusion kurtosis tensors," *Journal of Computational and Applied Mathematics (in press),* vol. doi:10.1016/j.cam.2007.10.012, 2007.

[19] P. J. Basser and C. Pierpaoli, "Microstructural and physiological features of tissues elucidated by quantitative-diffusion-tensor MRI," *J Magn Reson B,* vol. 111, pp. 209-19, Jun 1996.

[20] D. K. Jones, M. A. Horsfield, and A. Simmons, "Optimal strategies for measuring diffusion in anisotropic systems by magnetic resonance imaging," *Magn Reson Med,* vol. 42, pp. 515-25, Sep 1999.

[21] S. W. Sun, J. J. Neil, and S. K. Song, "Relative indices of water diffusion anisotropy are equivalent in live and formalin-fixed mouse brains," *Magn Reson Med,* vol. 50, pp. 743-8, Oct 2003.

[22] S. W. Sun, J. J. Neil, H. F. Liang, Y. Y. He, R. E. Schmidt, C. Y. Hsu, and S. K. Song, "Formalin fixation alters water diffusion coefficient magnitude but not anisotropy in infarcted brain," *Magn Reson Med,* vol. 53, pp. 1447-51, Jun 2005.

[23] C. Beaulieu, "The basis of anisotropic water diffusion in the nervous system - a technical review," *NMR Biomed,* vol. 15, pp. 435-55, Nov-Dec 2002.

[24] S. G. Waxman, J. D. Kocsis, and P. K. Stys, *The Axon : structure, function, and pathophysiology*. New York: Oxford University Press, 1995.